

Loss-of-function mutation of the *SCN3B*-encoded sodium channel β 3 subunit associated with a case of idiopathic ventricular fibrillation

Carmen R. Valdivia^{1†}, Argelia Medeiros-Domingo^{2,3,4†}, Bin Ye¹, Win-Kuang Shen⁵, Timothy J. Algers¹, Michael J. Ackerman^{2,3,4}, and Jonathan C. Makielski^{1*}

¹Department of Medicine, Cardiovascular Section, and the Cardiac Molecular Arrhythmias Research Program, University of Wisconsin-Madison, 600 Highland Avenue H6/349, Madison, WI 53792, USA; ²Department of Medicine, Division of Cardiovascular Diseases, Windland Smith Rice Sudden Death Genomics Laboratory, Mayo Clinic, Rochester, MN, USA; ³Department of Pediatrics, Division of Pediatric Cardiology, Windland Smith Rice Sudden Death Genomics Laboratory, Mayo Clinic, Rochester, MN, USA; ⁴Department of Molecular Pharmacology and Experimental Therapeutics, Windland Smith Rice Sudden Death Genomics Laboratory, Mayo Clinic, Rochester, MN, USA; and ⁵Division of Cardiovascular Diseases, Mayo Clinic, Rochester, MN, USA

Received 14 July 2009; revised 16 December 2009; accepted 21 December 2009; online publish-ahead-of-print 30 December 2009

Time for primary review: 16 days

Aims Loss-of-function mutations in the *SCN5A*-encoded sodium channel *SCN5A* or Nav1.5 have been identified in idiopathic ventricular fibrillation (IVF) in the absence of Brugada syndrome phenotype. Nav1.5 is regulated by four sodium channel auxiliary β subunits. Here, we report a case with IVF and a novel mutation in the *SCN3B*-encoded sodium channel β subunit Nav β 3 that causes a loss of function of Nav1.5 channels *in vitro*.

Methods and results Comprehensive open reading frame mutational analysis of *KCNQ1*, *KCNH2*, *SCN5A*, *KCNE1*, *KCNE2*, *GPD1L*, four sodium channel β subunit genes (*SCN1-4B*), and targeted scan of *RYR2* was performed. A novel missense mutation, Nav β 3-V54G, was identified in a 20-year-old male following witnessed collapse and defibrillation from VF. The ECG exhibited epsilon waves, and imaging studies demonstrated a structurally normal heart. The mutated residue was highly conserved across species, localized to the Nav β 3 extracellular domain, and absent in 800 reference alleles. We found that HEK-293 cells had endogenous Nav β 3, but COS cells did not. Co-expression of Nav1.5 with Nav β 3-V54G (with or without co-expression of the Nav β 1 subunit) in both HEK-293 cells and COS cells revealed a significant decrease in peak sodium current and a positive shift of inactivation compared with WT. Co-immunoprecipitation experiments showed association of Nav β 3 with Nav1.5, and immunocytochemistry demonstrated a dramatic decrease in trafficking to the plasma membrane when co-expressed with mutant Nav β 3-V54G.

Conclusion This study provides molecular and cellular evidence implicating mutations in Nav β 3 as a cause of IVF.

Keywords Na-channel • Sudden death • Ventricular arrhythmia • Inherited arrhythmia • Channel subunit

1. Introduction

Voltage-gated sodium channels play a fundamental role in many electrically excitable cells and tissues and more particularly in the contractile myocardium and specialized conduction tissue in the heart. Mutations causing loss of function of the Nav1.5 channel and decreasing peak sodium current (I_{Na}) are responsible for some forms of Brugada syndrome (BrS), idiopathic ventricular fibrillation (IVF), progressive cardiac conduction disease, autosomal recessive congenital sick sinus syndrome, atrial fibrillation, and dilated cardiomyopathy.

IVF is characterized by spontaneous ventricular fibrillation in the absence of structural heart disease (coronary/valvular heart disease, myocarditis, cardiomyopathy) and in the absence of well-defined electrophysiological diseases such as LQTS, BrS, and arrhythmogenic right ventricular cardiomyopathy/dysplasia (ARVC/D).¹ Three IVF-susceptibility genes have now been implicated (*SCN5A*, dipeptidyl-aminopeptidase-like protein 6 (*DPP6*), and *KCNJ8*).^{2–4} The first to be described were loss-of-function mutations in *SCN5A* where an IVF phenotype was noted in the absence of BrS features.² Recently, *DPP6*, which modulate transient outward current kinetics, was

[†]C.R.V. and A.M.-D. are co-equal first authors.

* Corresponding author. Tel: +1 608 263 9648; fax: +1 608 263 0405. Email: jcm@medicine.wisc.edu

Published on behalf of the European Society of Cardiology. All rights reserved. © The Author 2009. For permissions please email: journals.permissions@oxfordjournals.org.

reported in a familial IVF pedigree.³ Also, a mutation in the *KCNJ8*-encoded pore-forming subunit, Kir6.1, of the ATP-sensitive potassium channel was recently reported in a young female with IVF,⁴ but the functional effects of this mutation were not investigated. Here, we report the initial human mutation in the *SCN3B*-encoded sodium channel Nav β 3 subunit from a patient diagnosed clinically with IVF and show that it causes decreased I_{Na} as evidence for a plausible cause of the arrhythmia.

2. Methods

2.1 Mutational analysis

Comprehensive open reading frame/splice site mutational analysis of *KCNQ1*, *KCNH2*, *SCN5A*, *KCNE1*, *KCNE2*, *SCN1B*, *SCN2B*, *SCN3B*, *SCN4B*, and targeted *RYR2* was performed using polymerase chain reaction (PCR), denaturing high-performance liquid chromatography (DHPLC), and direct DNA sequencing as described previously.⁵ The study was performed according to the terms required by the Mayo Foundation Institution Review Board and conforms to the Declaration of Helsinki. Written informed consent was obtained from all participants (IRB protocol 1216-97).

2.2 Clones, site-directed mutagenesis, and cell lines

Nav β 3 (GenBank Acc no. NM_018400) was cloned from human heart mRNA (Clontech, Palo Alto, CA, USA) with RT-PCR and two primers: 5-ATGCCTGCCTTCAATAGATTG-3 and 5-CTATTCCTCCACTGGT ACC-3, then subcloned into the eukaryotic expression vectors pcDNA3 (Invitrogen, Carlsbad, CA, USA) and IRES-GFP, and confirmed by DNA sequencing analysis (Biotech Center of the University of Wisconsin-Madison). The cDNA of voltage-gated sodium channel alpha subunit gene, *SCN5A* (GenBank Acc. no. AY148488) was also subcloned into pcDNA3 vector (Invitrogen), and both were transiently transfected into HEK-293 cells at 1:1 ratio using Fugene (Roche). The novel missense mutation, Nav β 3-V54G, was engineered into the Nav β 3-WT by site-directed mutagenesis using QuikChange site-directed mutagenesis kit (Stratagene). For co-immunoprecipitation (co-IP) experiments, the FLAG peptide of DYKDDDDK was incorporated into *SCN5A* at the extracellular linker of DI between S1-2 and confirmed by sequencing.

2.3 I_{Na} measurement

I_{Na} from HEK-293 or COS cells co-expressing *SCN5A* with WT- and/or Nav β 3-V54G, and/or WT-Nav β 1 or an empty vector were recorded using the whole-cell configuration of the patch clamp technique using an Axopatch 200B amplifier and pClamp8.0 and data were acquired and analysed using software (Axon Instruments, Foster City, CA, USA) as described previously.⁶ I_{Na} was normalized to cell capacity and reported as pA/pF. The electrophysiological recordings were carried out at room temperature. The bath (extracellular) solution contained (in mM): NaCl 140, KCl 4, CaCl₂ 1.8, MgCl₂ 0.75, HEPES 5 (pH 7.4 set with NaOH). The pipette (intracellular) solution contained: CsF 120, CsCl 20, EGTA 2, HEPES 5 (pH 7.4 set with CsOH).

2.4 Co-immunoprecipitation

A rabbit polyclonal anti-Nav β 3 antibody was generated against residues 65–83 of the Nav β 3 (YenZym Antibodies, LLC, South San Francisco, CA, USA). Co-IP between *SCN5A* and Nav β 3 was performed using mouse heart and cell lysates from HEK-293 cells co-expressing the *SCN5A* tagged with a Flag epitope and the Nav β 3-WT or the Nav β 3-V54G. HEK-293 cells were lysed in RIPA buffer (25 mM Tris-HCl at pH 7.4, 150 mM NaCl, 1% Triton X-100, 1% sodium deoxycholate, 0.1% SDS, 5 mM EDTA, 1 mM DTT) containing complete protease

inhibitor cocktail (Roche, Basel, Switzerland). The preparation was immunoprecipitated with 1 μ g of Nav β 3 rabbit antibody (Zymed laboratories) or anti-Flag antibody (Sigma-Aldrich), and then electrophoretically separated by 4–20% SDS-PAGE and transferred into PVDF membranes for immunoblotting with either of the following antibodies: Nav1.5 antibody (Upstate Laboratory), anti-Flag-M2 antibody (Sigma), or anti-Nav β 3 antibody. Complexes were developed using the ECL-plus kit (Amersham Biosciences).

2.5 Immunocytochemistry

HEK-293 cells were transfected with *SCN5A* and the WT or Nav β 3-V54G and after 24 h, the cells were fixed with 4% paraformaldehyde, permeabilized with 0.1% Triton, and quenched with glycine. The cells were then blocked for 30 min with buffer (10% goat serum and 5 mM NaN₃-PBS) and incubated with the primary antibodies mouse anti-Flag-M2 (Sigma) against the Flag-tagged *SCN5A* and rabbit anti-Nav β 3 for 1 h at 37°C at 1:1000 dilution. The cells were washed three times for 10 min with washing buffer and incubated with secondary antibodies: Alexa 488 and Alexa 568 anti-mouse and anti-rabbit, respectively (Molecular Probes, Eugene, OR, USA) for 30 min at 37°C at 1:500 dilution, then washed three times for 10 min. The fluorescent labelled HEK-293 cells were viewed using a confocal imaging system FLUOVIEW 1000 mounted on an inverted microscope (Olympus). A 60 \times oil-immersion lens with a Kalman collection filter with two frames per image was used to record images. Z series were created by sequential scanning of green and red at 0.5 mm steps.

2.6 Live-cell western technique

COS cells expressing only empty vector or co-expressing *SCN5A* and Nav β 3-WT or Nav β 3-V54G were plated into collagen-coated 35 mm tissue culture plates and cultured overnight. For imaging, the cell culture media (MEM with 10% foetal bovine serum) was supplemented for 1 h with a primary anti-Flag antibody (1:500) at 37°C. The cells were washed for 10 min three times with cell culture media at 37°C. The cells were then cultured for 1 h in the secondary antibody IRDye 800 goat anti-mouse (1:500) (Li-cor Biosciences, Lincoln, NE, USA) at 37°C. Cells were then washed once in PBS for 10 min. The cells were imaged using the Li-cor Odyssey infrared imaging system (Li-cor Biosciences) and the intensity of the 800 nm infrared signal for each well was quantified using the Li-cor Odyssey infrared imaging system software. The mean intensity of a plate that contain untransfected cells was subtracted from the intensity of plates with cells expressing *SCN5A* + vector, *SCN5A* + Nav β 3-WT, *SCN5A* + Nav β 3-V54G, or *SCN5A* + both Nav β 3-WT and -V54G (1:1) to correct for any background signal not related to Flag staining.

2.7 Data analysis

Summary data are shown as the mean \pm standard error of the mean. Statistical significance was determined by using a Student's *t*-test for comparisons of two means or, when appropriate, analysis of variance (ANOVA) for comparisons of multiple means. A *P*-value of <0.05 was considered statistically significant.

3. Results

3.1 Clinical case

In 2001, a 20-year-old otherwise healthy male suddenly lost consciousness while playing basketball as his sentinel cardiac event. The emergency response team found him in ventricular fibrillation, and he was defibrillated rapidly and successfully on the basketball court and recovered fully with no neurological sequelae. He had no prior syncopal spells, and there was no history of sudden death in his family. After

comprehensive cardiological evaluation both locally and after referral to Mayo Clinic, the only peculiarity noted was an epsilon wave on 12-lead ECG (Figure 1). However, the T waves were not inverted in the right precordial leads, and there was no other evidence to suggest ARVC/D. Specifically, there was no ectopy on ambulatory recording or late potentials on signal-averaged ECG, and the echocardiogram was normal with no structural cardiac disease. In addition, a cardiac CT scan with and without contrast was unremarkable with no fatty infiltration of the right ventricle, aneurysmal dilatation, right ventricular enlargement, or dysfunction noted. With these negative findings, a right ventricular biopsy for ARVC was considered to be low yield for the risk. Besides ARVC/D and other cardiomyopathies, other possible cardiac conditions (anomalous coronary arteries, long QT syndrome, BrS, and catecholaminergic polymorphic ventricular tachycardia) were evaluated and excluded by a negative coronary angiogram, negative epinephrine QT stress test, negative procainamide challenge, and negative electrophysiology study with and without isoproterenol. An ICD was implanted without complication. The patient returned for follow-up 1 year later for repeat imaging studies and once again the contrast CT scan was unremarkable. No subsequent events have occurred after 8 years of follow-up.

3.2 Mutational analysis

Mutational analysis of the RYR2 and LQTS genes (*KCNQ1*, *KCNH2*, *SCN5A*, *KCNE1*, and *KCNE2*) did not yield putative arrhythmia mutations. A T to G base substitution at position 161 was identified in *SCN3B* which yielded a missense mutation V54G [valine (V) to glycine (G) at position 54] (Figure 2A). This mutation was absent in 800 references alleles. V54G was localized to the extracellular region of the Navβ3 subunit and involves a highly conserved residue across species (Figure 2B and D). The proband's mother

hosted the mutation and was asymptomatic, but notably also displayed 'J' point elevation on his 12-lead ECG (Figure 2C).

3.3 Navβ3-V54G and I_{Na}

Representative I_{Na} traces from HEK-293 cells expressing SCN5A co-expressed with a blank vector control, Navβ3-WT, or Navβ3-V54G (Figure 3A) show that the mutation markedly decreased peak I_{Na} density, and summary data (Figure 3B) show that this decrease was statistically significant. Summary plots of the current–voltage relationship normalized to peak (Figure 4A and Table 1) show that Navβ3-V54G caused a depolarizing shift of the voltage dependence of activation compared with Navβ3-WT, but not to SCN5A + vector; this effect may have contributed to the decreased I_{Na} density. In HEK-293 cells, but not COS cells, Navβ3-WT caused a 4 mV negative shift in the midpoint of inactivation compared with SCN5A + vector, and this effect was lost in the presence of Navβ3-V54G (Figure 4B and Table 1). These data are consistent with changes in kinetics that result in a 'loss of function' by Navβ3-V54G. No changes were observed for late persistent I_{Na} (Table 1).

3.4 Navβ3 associates with Nav1.5

We developed a Navβ3 antibody with the epitope targeted to the extracellular domain of Navβ3. The antibody gave bands at the expected molecular weight for Navβ3-WT and Navβ3-V54G expressed in COS cells, but not for the Navβ1, Navβ2, or Navβ4 subunits of the sodium channel (data not shown), suggesting that the antibody was specific for the Navβ3 subunit over other highly homologous sodium channel β subunits. Interestingly, we detected a band for Navβ3 in non-transfected HEK-293 cells, the standard cell line used for studies of SCN5A, but not in COS cells (data not shown). To determine whether SCN5A and Navβ3 are associated, we performed co-IP experiments by immunoprecipitating with the Navβ3 antibody and probing for SCN5A with Nav1.5 antibody or

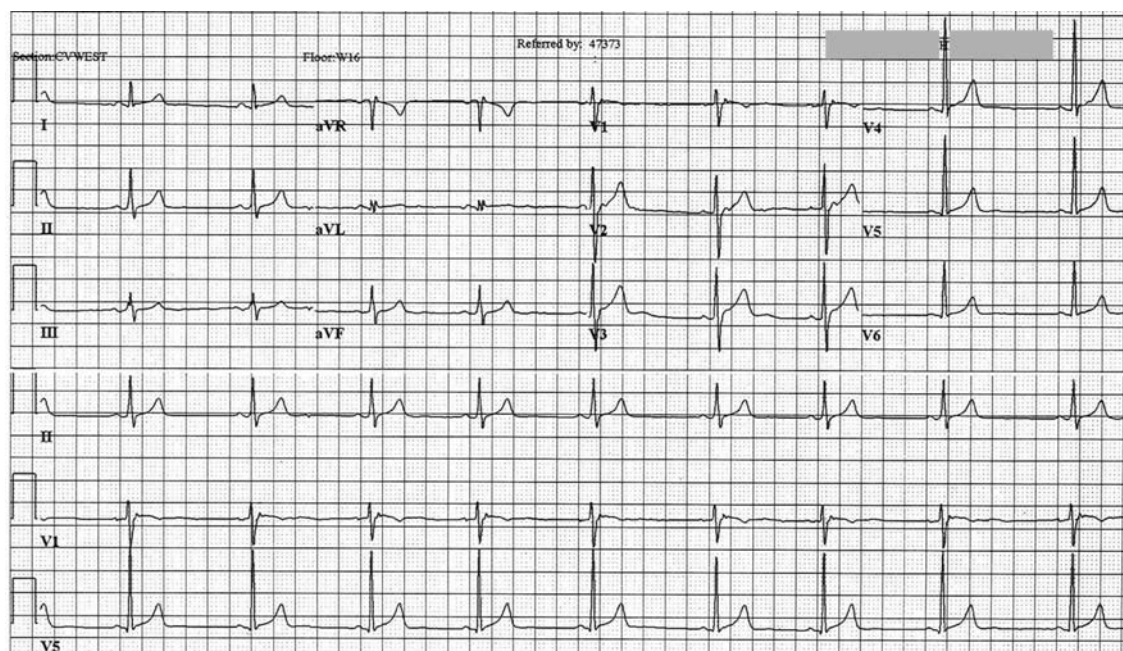


Figure 1 Twelve-lead ECG of the 20-year-old index case showing sinus rhythm, QRS axis within normal limits. Epsilon waves are evident in leads V1, V2, and V3.

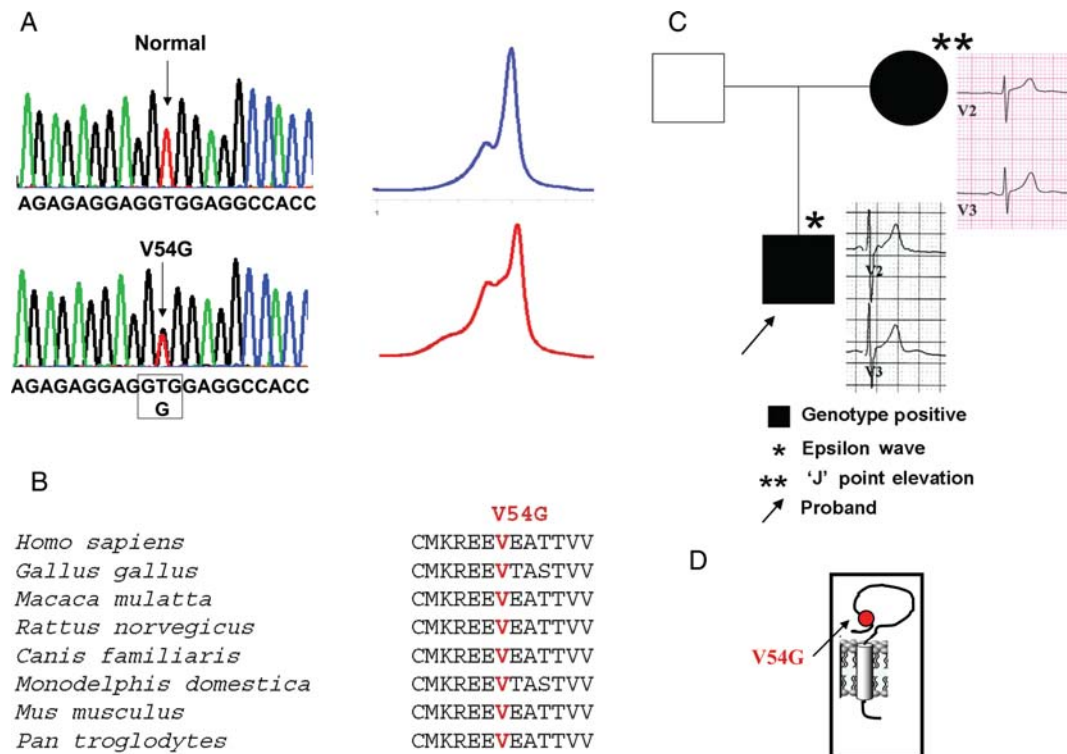


Figure 2 (A) Left: Proband DNA sequence chromatogram showing a T > G substitution generating a valine (V) to glycine (G) substitution at residue 54 of Navβ3. Right: Wild-type DHPLC profile in blue colour, mutant, and aberrant profile in red colour. (B) Navβ3-V54G mutant involves residue that is highly conserved across different species. (C) Pedigree and ECG of the affected family. Black symbol: genotype positives. The ECG of the Navβ3-V54G mutation carriers is shown next to the symbol. The proband exhibits epsilon waves while the mother exhibits 'J point' elevation. (D) Predicted location of the Navβ3-V54G mutation in the extracellular domain of the Navβ3 subunit.

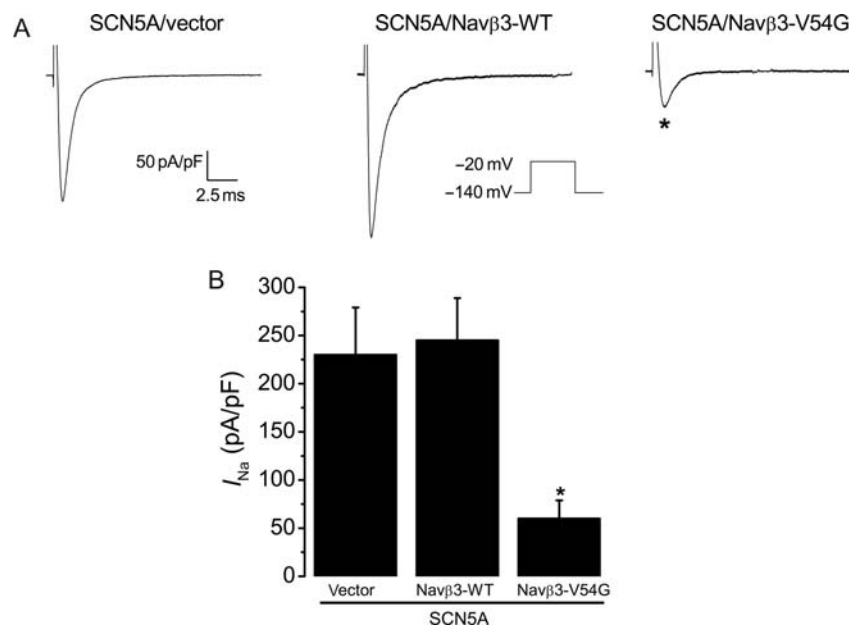


Figure 3 Navβ3-V54G reduced I_{Na} in HEK-293 cells (A) Whole-cell current traces from representative cells expressing SCN5A + vector, SCN5A co-expressed with β3-WT or Navβ3-V54G 24 h after transfection. I_{Na} was elicited from a step depolarization of -20 mV from a holding potential of -140 mV (see inset). (B) Summary data for I_{Na} density for test potential to -20 mV. Number of cells $n = 13-26$ as indicated in Table 1. * $P < 0.05$ vs. Navβ3-WT and vector.

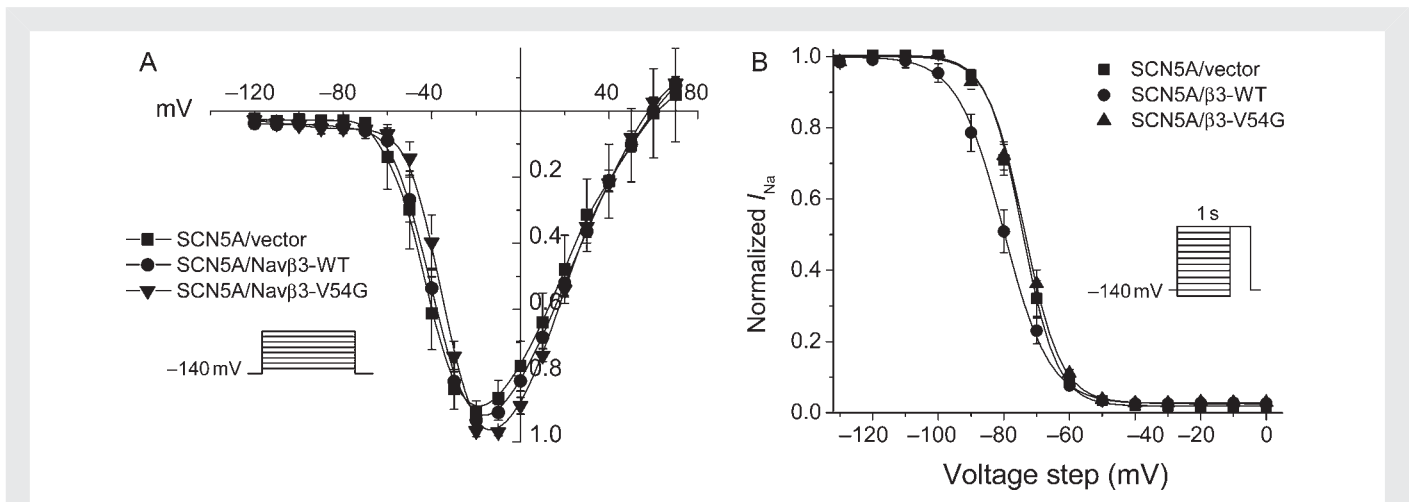


Figure 4 Navβ3-WT shifted inactivation kinetics, but Navβ3-V54G did not. (A) Peak current–voltage plot of summary I_{Na} normalized to the maximal I_{Na} in response to a series of depolarizations from a holding potential of -140 mV. (B) Summary steady-state inactivation relationship in response to a 1 s conditioning voltage step. The lines represent a fit to the Boltzmann function: $I_{Na} = I_{Na-max}[1 + \exp((V_c - V_{1/2})/\kappa)]^{-1}$, where the $V_{1/2}$ and κ are the midpoint and the slope factor, respectively, and V_c is the membrane potential. Parameters of the fit in Table 1 show a significant depolarizing shift for activation by Navβ3-V54G compared with Navβ3-WT and a significant hyperpolarizing shift for inactivation by Navβ3-WT compared with SCN5A + vector or Navβ3-V54G.

Table 1 Kinetics of SCN5A + β3 in HEK-293 cells

	Peak I_{Na}		Activation			Inactivation		Recovery			I_{NaL}		
	pA/pF	n	$V_{1/2}$ (mV)	K	n	$V_{1/2}$ (mV)	n	τ_f (ms)	τ_s (ms)	As (%)	n	%	n
SCN5A + vector	-230 ± 49	13	-36 ± 2	4.7	7	-75 ± 1	9	1.5 ± 0.3	54 ± 9	25 ± 2	8	0.28 ± 0.05	10
SCN5A + Navβ3-WT	-245 ± 44	26	-39 ± 1	4.7	22	$-79 \pm 1^{\#}$	20	1.4 ± 0.2	44 ± 7	24 ± 2	14	0.46 ± 0.04	15
SCN5A + Navβ3-V54G	$-60 \pm 19^*$	14	$-35 \pm 1^*$	5.1	10	$-75 \pm 1^*$	8	1.1 ± 0.2	60 ± 10	22 ± 1	4	0.38 ± 0.07	8

$^{\#}P < 0.05$ vs. SCN5A + vector.

$^*P < 0.05$ vs. Navβ3-WT.

anti-Flag antibody (Figure 5). In HEK-293 cells co-expressing SCN5A and Navβ3-WT (Figure 5A, lane 4), the Navβ3 subunit antibody co-immunoprecipitated SCN5A, and it also co-immunoprecipitated SCN5A when SCN5A was expressed alone (Figure 5A, lane 3), consistent with the finding that HEK-293 cells have endogenous Navβ3 subunits. SCN5A was also co-immunoprecipitated by Navβ3 in homogenates obtained from adult cardiac myocytes from mouse (Figure 5A, lane 1), but the signal for SCN5A in neonatal mouse myocytes was very weak, consistent with a reported absence of Navβ3 subunits at this stage.⁷ Co-expressing Navβ3-WT or Navβ3-V54G and the Flag-tagged SCN5A in COS cells also co-immunoprecipitated the complex.

3.5 Navβ3-V54G caused an SCN5A trafficking defect

The location of co-expressed SCN5A and Navβ3 subunits was investigated in HEK-293 cells by immunocytochemistry and confocal microscopy. The SCN5A location was visualized by expressing an SCN5A-Flag construct and probing with a Flag antibody (green signal) (Figure 5D, b and f), and the Navβ3 subunit was probed using the native antibody (red signal) (Figure 5D, c and g). For Navβ3-WT

(Figure 5D, top panels), both SCN5A and Navβ3-WT localized at the plasma membrane. However, Navβ3-V54G caused a marked decrease in the cell surface signal for both SCN5A and Navβ3 (Figure 5D, bottom panels). These results suggest that Navβ3-V54G caused retention of the two subunits and accounted for the decrease in I_{Na} density in the presence of Navβ3-V54G.

3.6 β3-V54G and I_{Na} in COS cells

Although HEK-293 cells are the standard heterologous cell line for the study of SCN5A, our observation that HEK-293 cells have endogenously expressing Navβ3 prompted us to also study the effects of the Navβ3 subunit on SCN5A in COS cells which we have showed lack the endogenous Navβ3 subunit. Representative I_{Na} traces from COS cells co-expressing SCN5A and one of the following plasmids: a blank vector control, Navβ3-WT, Navβ3-V54G, or both Navβ3-WT and Navβ3-V54G at 1:1 ratio (Figure 6A and Table 2). In these cells, Navβ3-WT caused an increase in I_{Na} density, non-significant compared with SCN5A alone, and Navβ3-V54G had a profound and significant suppressive effect on I_{Na} density. When Navβ3-WT was co-expressed with

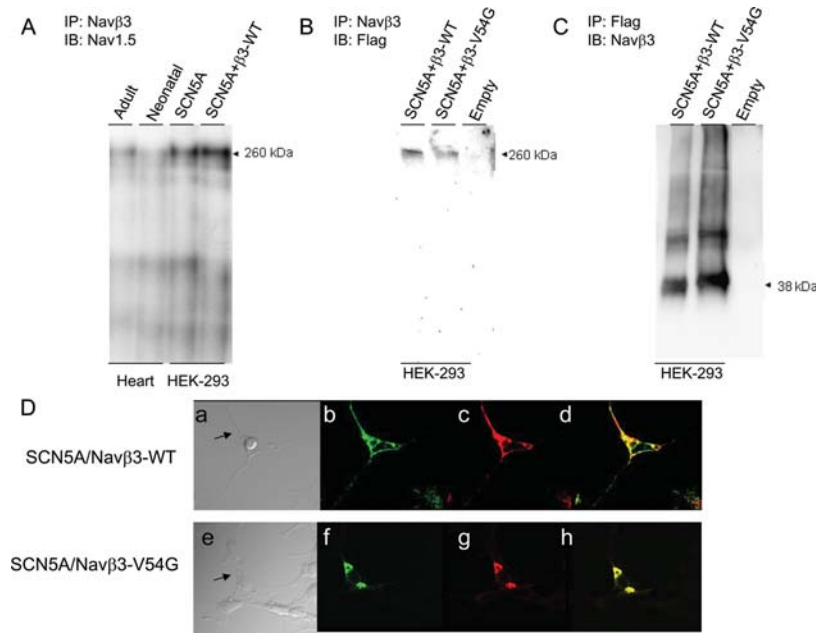


Figure 5 Co-IP of SCN5A and Navβ3 subunits. (A) Heart homogenates were obtained from adult or neonatal mouse hearts, and from cell lysates obtained from HEK-293 cells expressing SCN5A alone or cells co-expressing SCN5A and Navβ3. (B and C) Cell lysates obtained from HEK-293 cells co-expressing SCN5A Flag-tagged and Navβ3-WT or Navβ3-V54G. Complexes were precipitated with Navβ3 or Flag antibodies (as in 2) and immunoblotted with either anti-Nav1.5, anti-Flag, or anti-Navβ3 antibody. The Nav1.5 antibody and the anti-FLAG antibody recognize the 260 kDa SCN5A α subunit (A and B) and the Navβ3 antibody recognizes the 38 kDa Navβ3 subunit (C), the bands above 38 kDa are signals for the IgG binding. (D) Navβ3-V54G prevents trafficking of SCN5A to the cell surface. HEK-293 cells were transfected 1:1 ratio with SCN5A and Navβ3-WT or Navβ3-V54G and subjected to immunolabelling 24 h after transfection. The cells were incubated with the primary antibodies mouse anti-Flag-M2 against the Flag-tagged SCN5A and the rabbit anti-Navβ3 against Navβ3. After washes, the cells were incubated with secondary antibodies: Alexa 488 and Alexa 568, anti-mouse and anti-rabbit, respectively. The fluorescent-labelled HEK-293 cells were viewed and scanned using a confocal imaging system Fluoview 1000. The Z series were created by sequential scanning of green and red at 0.5 mm steps. The transmittance image (panels a and e), the Flag-SCN5A imaging (panels b and f), the red Navβ3 imaging (panels c and g), and merge (panels d and h).

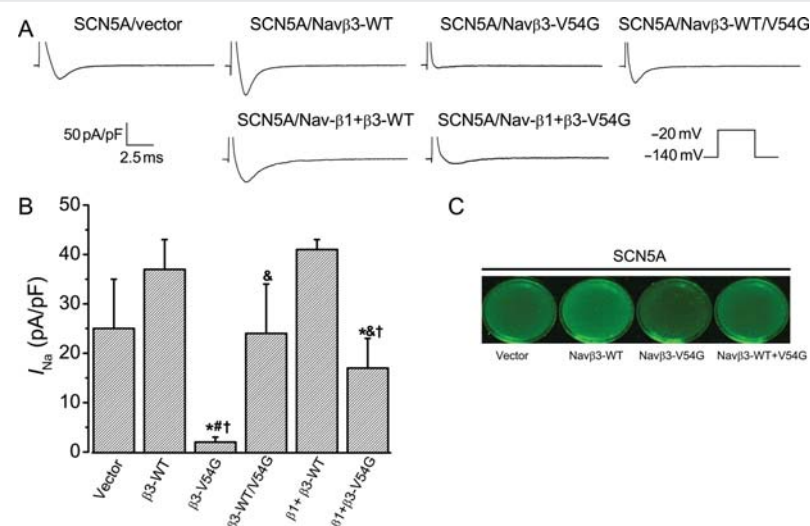


Figure 6 Navβ3-V54G reduced I_{Na} in COS cells. Equal amounts of blank vector, Navβ3-WT or Navβ3-V54G, and in some cells Navβ1-WT were co-transfected with SCN5A in COS cells for a total amount of 1.5 μg DNA. (A) Whole-cell current traces from representative COS cells co-expressed with SCN5A + vector, SCN5A + Navβ3-WT, SCN5A + Navβ3-V54G, SCN5A + Navβ3-WT, and -V54G with and without Navβ1-WT measured 24 h after transfection. I_{Na} was elicited from a step depolarization of -20 mV from a holding potential of -140 mV (see inset). (B) Summary data for I_{Na} density for test potential to -20 mV, experiment number $n = 6-12$. # $P < 0.05$ vs. vector, * $P < 0.05$ vs. Navβ3-WT, † $P < 0.05$ vs. Navβ1 + Navβ3-WT, & $P < 0.05$ vs. Navβ3-V54G. (C) COS cells co-expressing SCN5A and Navβ3 plasmids were subjected to live-cell western blot, plates show the signal from the secondary anti-mouse antibody-labelled IRDye 800, and detected on an infrared imaging system (Odyssey). An un-transfected plate was used to subtract the background from each plate.

Table 2 Kinetics of SCN5A + β 1-WT and β 3 in COS cells

	Peak I_{Na}		Activation			Inactivation		Recovery			
	pA/pF	n	$V_{1/2}$ (mV)	K	n	$V_{1/2}$ (mV)	n	τ_f (ms)	τ_s (ms)	As (%)	n
SCN5A + vector	-25 ± 10	10	-34 ± 3	4.8	6	-74 ± 1	9	2.1 ± 0.5	29 ± 9	31 ± 4	4
SCN5A + Nav β 3-WT	-37 ± 6	12	-36 ± 1	5.1	8	-75 ± 1	7	2.1 ± 0.1	36 ± 9	$20 \pm 4^{\#}$	4
SCN5A + Nav β 1, β 3-WT	-41 ± 2	8	-34 ± 3	5.1	7	-77 ± 3	7	2.1 ± 0.3	49 ± 24	$21 \pm 4^{\#}$	5
SCN5A + Nav β 3-V54G	$-2 \pm 1^{\#\dagger}$	6	N/A			N/A		N/A	N/A	N/A	
SCN5A + Nav β 1, β 3-V54G	$-17 \pm 6^{*\dagger\&}$	10	$-32 \pm 2^*$	5.1	7	-75 ± 1	8	2.8 ± 0.3	62 ± 27	22 ± 4	6
SCN5A + β 3-WT/V54G	$-24 \pm 10^{\&}$	6	$-30 \pm 1^*$	5.3	4	-73 ± 1	3	—	—	—	—

$\#P < 0.05$ vs. SCN5A + vector.

$*P < 0.05$ vs. Nav β 3-WT.

$\dagger P < 0.05$ vs. Nav β 1 + β 3-WT.

$\&P < 0.05$ vs. Nav β 3-V54G.

Nav β 3-V54G, the I_{Na} density was not significantly different from Nav β 3-WT. Summary of the I_{Na} density in each group is shown (Figure 6B and Table 2). In addition, co-expression with SCN5A, Nav β 1 and Nav β 3-WT, or Nav β 3-V54G had no significant additional effects on kinetics (Table 2). In COS cells co-expressing the Nav β 1 and Nav β 3-WT, the levels of I_{Na} density were similar than in the absence of Nav β 1. However, for Nav β 3-V54G, the presence of the Nav β 1 'partially rescues' the decrease in I_{Na} density (Figure 6A and B).

3.7 SCN5A cell surface expression in COS cells by live-cell western technique

This relatively new technique provided a tool to quantitatively measure cell surface expression of SCN5A by imaging living cells attached at the bottom of 35 mm tissue culture plates. Here, COS cells co-expressing SCN5A Flag-tagged and Nav β 3 plasmids as in Figure 6A and B were subjected to live-cell western blot using the anti-Flag antibody, then the signal was detected by a secondary anti-mouse antibody labelled with an infrared dye (IRDye 800), and detected on an infrared imaging system (Odyssey). Figure 6C shows the infrared signal at 800 nm wave length, and each plate has a confluent layer of COS cells with good transfection efficiency as indicated by GFP expression. A non-transfected plate was used to subtract the background from each plate containing cells expressing the SCN5A and the Nav β 3 constructs. The infrared imaging analysis software quantifies the infrared signal (pixels count) within a pre-defined area (mm^2), and Figure 6C shows the relative mean infrared signal intensities. The live-cell western technique is consistent with and corroborates the loss-of-function/trafficking-defective findings from the whole cell patch clamp and immunocytochemical analyses.

4. Discussion

4.1 IVF ECG pattern

The patient described in this report had documented spontaneous ventricular fibrillation in the absence of structural heart disease or other well-defined electrophysiological diseases such as LQTS, BrS, or ARVC/D. IVF cases are often recognized and studied only after their first out-of-hospital cardiac arrest. A lack of specific electrocardiographic markers makes identification of pre-disposed individuals

challenging. The ECG is often normal or does not provide sufficiently specific findings for clinical diagnosis in asymptomatic cases at risk of ventricular fibrillation.^{8,9} The patient's only electrocardiographic/structural peculiarity was the manifest epsilon wave in the right precordial leads of V1, V2, and V3 (Figure 1). The epsilon wave has been described in ARVC/D; however, our patient lacked other ECG findings often described in ARVC/D, such as T-wave inversion in anterior precordial leads, ventricular conduction delay, ventricular axis deviation, ectopy on Holter, and late potentials.^{10,11} Moreover, no structural or haemodynamic abnormalities were found by either echocardiography or CT scan. This case was diagnosed clinically as IVF and did not meet criteria for AVRC/D, but the implications of these findings may require reinterpretation should additional cases be found that more resemble AVRC/D.

Interestingly, his mother is an asymptomatic gene-mutation carrier and exhibited J-point elevation in her ECG. This early repolarization pattern previously thought to be a normal variant, may be a marker of life-threatening ventricular arrhythmias⁸ present in 31% of IVF, and J-point elevation was also a frequent observation in patients with IVF.⁹ These patterns, however, are also frequently observed in 'normal' subjects, as many as 7% of young athletes,¹² and it is therefore a very non-specific marker for IVF predisposition. A possible overlap of BrS and IVF and association with early repolarization extends to the molecular level, where mutations in SCN5A that cause loss of function of I_{Na} have been associated with both IVF^{2,13} as well as BrS, and also electrogenesis of the early repolarization pattern.¹⁴ Our finding that Nav β 3-V54G causes loss-of-function I_{Na} provides a plausible mechanism for IVF consistent with a molecular phenotype of loss of I_{Na} function previously associated with IVF, BrS, and early repolarization.¹⁴

4.2 Nav β 3 subunit and I_{Na}

The α subunit of the voltage-dependent Na channel associates with four smaller Nav β subunits (Nav β 1, Nav β 2, Nav β 3, and Nav β 4), which play critical roles in cell adhesion, signal transduction, channel expression at the plasma membrane, and voltage dependence of the channel gating. The Nav β subunits have been implicated previously in arrhythmia syndromes: altered interaction between the Nav β 1 subunit and a mutated α subunit has been proposed as a mechanism for BrS,¹⁵ and mutations in the Nav β 1 subunit itself have been

described recently in BrS and conduction disease.¹⁶ Mutations in the Navβ4 subunit have been found in LQTS.¹⁷ Previous to this report, mutations in Navβ2 and Navβ3 have not been implicated in human arrhythmia, but interestingly, a transgenic mouse lacking the Navβ3 subunit exhibited susceptibility to ventricular arrhythmias¹⁸ and altered conduction¹⁹ very similar to that of a transgenic mouse model with decreased I_{Na} ,²⁰ and a mutation in *SCN3B* has been reported in a patient with an ECG pattern consistent with BrS.²¹

Navβ3 is expressed in ventricles and Purkinje cells²² and share 57 and 47% homology with Navβ1 and Navβ2, respectively. The co-IP data of the Navβ3 subunit and SCN5A (Figure 5) in both heterologous systems and native tissue support a direct or indirect physical association in addition to the functional effects (Figures 3 and 4). The reported effects of the Navβ3 subunit on I_{Na} vary depending upon the cell preparation (oocytes vs. somatic cells) and the sodium channel isoform used. We observed a hyperpolarizing effect on Nav1.5 inactivation in HEK-293 cells, which agrees with the Navβ3-mediated shift reported in I_{Na} from rat brain cells,²³ Nav1.3 channels in CHO cells,²⁴ Nav1.2 and Nav1.8 in oocytes (but no shift with Nav1.4),²⁵ and on Nav1.5 in CHO cells.²⁶ In contrast to our results, one study showed a depolarizing shift with Nav1.5 in oocytes.²² Navβ3 knockout mouse¹⁸ ventricular myocytes showed a hyperpolarizing shift in the knockout, suggesting that in the mouse heart *in vivo*, the effect of Navβ3 is also a depolarizing shift. In the knockout, however, levels of the Navβ1 subunit and the α subunit were measured and altered, and other unexamined secondary changes could have been present, so the pure effect of Navβ3 might differ from the results observed in the knockout mouse. Although altered kinetics is potentially important for function, the more dramatic effect observed by the Navβ3 subunit was an increase in I_{Na} density that was also observed with co-expression of SCN5A in oocytes,²² and consistent with the decrease in I_{Na} observed in myocytes of the Navβ3 knockout mouse.¹⁸

4.3 β3-V54G caused SCN5A (Nav1.5) loss of function

The Navβ3-V54G mutation reduced I_{Na} by >70% in HEK-293 cells (Figure 3) and by >90% in COS cells (Figure 6) compared with Navβ3-WT. Also, Navβ3-V54G did not cause the hyperpolarizing shift in inactivation induced by Navβ3-WT (Figure 4B). Both of these are consistent with a loss of the Navβ3-WT functional effects on I_{Na} . Fluorescent immunocytochemistry (Figure 5D) suggests that the mechanism for the decreased I_{Na} is a decreased expression of both the Navβ3 subunit and SCN5A at the cell surface. The detailed mechanisms for the effect, however, remained unclear. We discovered that HEK-293 cells express the Navβ3 subunit endogenously, whereas COS cells do not. This could account for the finding that overexpression of Navβ3-WT showed a non-significant increase in I_{Na} in HEK-293 cells. However, in COS cells, Navβ3-WT showed a non-significant trend for increased I_{Na} (Figures 3 and 6), consistent with endogenous Navβ3-WT effects in HEK-293 cells.

The patient was heterozygous for the mutation. We attempted to recapitulate this *in vitro* by co-expression of Navβ3-V54G with Navβ3-WT in COS cells. Here, we obtained a more highly variable reduction in I_{Na} density that did not reach significance, and we speculate that gene dosage may account for this discrepancy (data not shown). In addition, the effects *in vivo* may depend upon specific interactions with other subunits such as the Navβ1 subunit,^{26,27} although

our co-expression studies with Navβ1 (Figure 6 and Table 2) suggest little effect on the Navβ3-WT, but a 'partial rescue' for the Navβ3-V54G. The extracellular domain of the Navβ3 exerted an important influence on channel kinetics, and the intracellular domain was important for targeting the channel to the surface membrane in one study.²⁸ But, Navβ3-V54G in the extracellular domain had a profound effect on trafficking in our study, and this is consistent with a mutation Navβ3-L10P in the extracellular domain associated with loss of I_{Na} density in a BrS patient.²¹ The overall findings *in vitro*, however, are consistent with Navβ3-V54G being an ineffective chaperone for SCN5A compared with Navβ3-WT, and even competing with Navβ3-WT for this function. More insight into detailed mechanisms awaits further study.

4.4 Summary, implications, and caveats

The clinical findings and the functional data reported here support the idea that the *SCN3B*-encoded Navβ3 subunit interacts with SCN5A α subunits creating a loss-of-function phenotype, and supports *SCN3B* as a novel IVF-susceptibility gene. The Navβ3-V54G mutation caused loss of the Navβ3 function and a reduction in I_{Na} , possibly by interfering with the chaperone and cell membrane localization functions of the Navβ3 subunit. The pedigree was not sufficient for genetic linkage analysis; therefore, the pathogenicity of this mutation rests upon its (i) absence in 800 reference alleles, (ii) involvement of a highly conserved residue, and (iii) a markedly perturbed molecular/cellular phenotype that yields the loss of function of I_{Na} , providing a plausible arrhythmogenic mechanism consistent with previously described IVF and BrS mutations. In addition, at this time, the finding is from a single case, and it will be interesting to determine whether mutations in *SCN3B* explain other cases of IVF, genotype-negative BrS, or autopsy-negative sudden unexplained death.

Conflict of interest: M.J.A. is a consultant for PGxHealth. Intellectual property derived from M.J.A.'s research program resulted in license agreements in 2004 between Mayo Clinic Health Solutions (formerly Mayo Medical Ventures) and PGxHealth (formerly Genaisance Pharmaceuticals).

Funding

This work was supported by the University of Wisconsin Cellular and Molecular Arrhythmia Research Program (J.C.M.) and the Mayo Clinic Windland Smith Rice Comprehensive Sudden Cardiac Death Program (M.J.A.), the Established Investigator Award from the American Heart Association (M.J.A.), and the National Institutes of Health HD42569 (M.J.A.) and HL71092 (J.C.M.).

References

- Zipes DP, Wellens HJ. Sudden cardiac death. *Circulation* 1998;**98**:2334–2351.
- Akai J, Makita N, Sakurada H, Shirai N, Ueda K, Kitabatake A et al. A novel SCN5A mutation associated with idiopathic ventricular fibrillation without typical ECG findings of Brugada syndrome. *FEBS Lett* 2000;**479**:29–34.
- Alders M, Koopmann TT, Christiaans I, Postema PG, Beekman L, Tanck MW et al. Haplotype-sharing analysis implicates chromosome 7q36 harboring DPP6 in familial idiopathic ventricular fibrillation. *Am J Hum Genet* 2009;**84**:468–476.
- Haissaguerre M, Chatel S, Sacher F, Weerasooriya R, Probst V, Loussoarn G et al. Ventricular fibrillation with prominent early repolarization associated with a rare variant of KCNJ8/KATP channel. *J Cardiovasc Electrophysiol* 2009;**20**:93–98.
- Tester DJ, Will ML, Ackerman MJ. Mutation detection in congenital long QT syndrome: cardiac channel gene screen using PCR, dHPLC, and direct DNA sequencing. *Methods Mol Med* 2006;**128**:181–207.

6. Valdivia CR, Ackerman MJ, Tester DA, Wada T, McCormack J, Ye B et al. A novel *SCN5A* arrhythmia mutation, M1766L, with expression defect rescued by mexiletine. *Cardiovasc Res* 2002;**54**:624–629.
7. Fahmi AI, Forhead AJ, Fowden AL, Vandenberg JI. Cortisol influences the ontogeny of both alpha- and beta-subunits of the cardiac sodium channel in fetal sheep. *J Endocrinol* 2004;**180**:449–455.
8. Haissaguerre M, Derval N, Sacher F, Jesel L, Deisenhofer I, de Roy L et al. Sudden cardiac arrest associated with early repolarization. *N Engl J Med* 2008;**358**:2016–2023.
9. Rosso R, Kogan E, Belhassen B, Rozovski U, Scheinman MM, Zeltser D et al. J-point elevation in survivors of primary ventricular fibrillation and matched control subjects: incidence and clinical significance. *J Am Coll Cardiol* 2008;**52**:1231–1238.
10. Marcus FI, Zareba W, Calkins H, Towbin JA, Basso C, Bluemke DA et al. Arrhythmogenic right ventricular cardiomyopathy/dysplasia clinical presentation and diagnostic evaluation: results from the North American Multidisciplinary Study. *Heart Rhythm* 2009;**6**:984–992.
11. Steriotes AK, Bauce B, Daliento L, Rigato I, Mazzotti E, Folino AF et al. Electrocardiographic pattern in arrhythmogenic right ventricular cardiomyopathy. *Am J Cardiol* 2009;**103**:1302–1308.
12. Pelliccia A, Culasso F, Di Paolo FM, Accettura D, Cantore R, Castagna W et al. Prevalence of abnormal electrocardiograms in a large, unselected population undergoing pre-participation cardiovascular screening. *Eur Heart J* 2007;**28**:2006–2010.
13. Wan X, Wang Q, Kirsch GE. Functional suppression of sodium channels by beta(1)-subunits as a molecular mechanism of idiopathic ventricular fibrillation. *J Mol Cell Cardiol* 2000;**32**:1873–1884.
14. Gussak I, Antzelevitch C. Early repolarization syndrome: clinical characteristics and possible cellular and ionic mechanisms. *J Electrocardiol* 2000;**33**:299–309.
15. Makita N, Shirai N, Wang DW, Sasaki K, George AL Jr, Kanno M et al. Cardiac Na⁺ channel dysfunction in Brugada syndrome is aggravated by β 1-subunit. *Circulation* 2000;**101**:54–60.
16. Watanabe H, Koopmann TT, Le Scouarnec S, Yang T, Ingram CR, Schott JJ et al. Sodium channel beta1 subunit mutations associated with Brugada syndrome and cardiac conduction disease in humans. *J Clin Invest* 2008;**118**:2260–2268.
17. Medeiros-Domingo A, Kaku T, Tester DJ, Iturralde-Torres P, Itty A, Ye B et al. SCN4B-encoded sodium channel β 4 subunit in congenital long-QT syndrome. *Circulation* 2007;**116**:136–142.
18. Hakim P, Gurung IS, Pedersen TH, Thresher R, Brice N, Lawrence J et al. *Scn3b* knockout mice exhibit abnormal ventricular electrophysiological properties. *Prog Biophys Mol Biol* 2008;**98**:251–266.
19. Hakim P, Brice N, Thresher R, Lawrence J, Zhang Y, Jackson AP et al. *Scn3b* knockout mice exhibit abnormal sino-atrial and cardiac conduction properties. *Acta Physiol (Oxf)* 2009;**198**:47–59.
20. Papadatos GA, Wallerstein PM, Head CE, Ratcliff R, Brady PA, Benndorf K et al. Slowed conduction and ventricular tachycardia after targeted disruption of the cardiac sodium channel gene *Scn5a*. *Proc Natl Acad Sci USA* 2002;**99**:6210–6215.
21. Hu D, Barajas Martinez B, Burashnikov A, Springer M, Wu Y, Varro A et al. A mutation in the beta3 subunit of the cardiac sodium channel associated with Brugada ECG phenotype. *Circ Cardiovasc Genet* 2009;**2**:270–278.
22. Fahmi AI, Patel M, Stevens EB, Fowden AL, John JE III, Lee K et al. The sodium channel beta-subunit *SCN3b* modulates the kinetics of *SCN5a* and is expressed heterogeneously in sheep heart. *J Physiol* 2001;**537**:693–700.
23. Morgan K, Stevens EB, Shah B, Cox PJ, Dixon AK, Lee K et al. beta 3: an additional auxiliary subunit of the voltage-sensitive sodium channel that modulates channel gating with distinct kinetics. *Proc Natl Acad Sci USA* 2000;**97**:2308–2313.
24. Meadows LS, Chen YH, Powell AJ, Clare JJ, Ragsdale DS. Functional modulation of human brain Nav1.3 sodium channels, expressed in mammalian cells, by auxiliary beta 1, beta 2 and beta 3 subunits. *Neuroscience* 2002;**114**:745–753.
25. Stevens EB, Cox PJ, Shah BS, Dixon AK, Richardson PJ, Pinnock RD et al. Tissue distribution and functional expression of the human voltage-gated sodium channel beta3 subunit. *Pflugers Arch* 2001;**441**:481–488.
26. Ko SH, Lenkowski PV, Lee HC, Mounsey JP, Patel MK. Modulation of Na(v)1.5 by beta1- and beta3-subunit co-expression in mammalian cells. *Pflugers Arch* 2005;**449**:403–412.
27. Vijayaragavan K, Powell AJ, Kinghorn IJ, Chahine M. Role of auxiliary beta1-, beta2-, and beta3-subunits and their interaction with Na(v)1.8 voltage-gated sodium channel. *Biochem Biophys Res Commun* 2004;**319**:531–540.
28. Yu EJ, Ko SH, Lenkowski PV, Pance A, Patel MK, Jackson AP. Distinct domains of the sodium channel beta3-subunit modulate channel-gating kinetics and subcellular location. *Biochem J* 2005;**392**:519–526.